TUDelft

Delft University of Technology

RSS-based sensor localization in underwater acoustic sensor networks

Xu, Tao; Hu, Yongchang; Zhang, Bingbing; Leus, Geert

Citation (APA)
Xu, T., Hu, Y., Zhang, B., & Leus, G. (2016). RSS-based sensor localization in underwater acoustic sensor networks. In M. Dong, & T. F. Zheng (Eds.), *2016 IEEE International Conference on Acoustics, Speech and Signal Processing (ICASSP): Proceedings* (pp. 3906-3910). IEEE. https://doi.org/10.1109/icassp.2016.7472409

Important note
To cite this publication, please use the final published version (if applicable).
Please check the document version above.

RSS-BASED SENSOR LOCALIZATION IN UNDERWATER ACOUSTIC SENSOR NETWORKS

Tao Xu[1,2], Yongchang Hu[3], Bingbing Zhang[4] and Geert Leus[3]

[1] Tianjin 712 Communication & Broadcasting Co. Ltd, Tianjin, 300462, China

[2] Institute of Microelectronics, Tsinghua University, 100084, Beijing, China

[3] Fac. EEMCS, Delft University of Technology, Mekelweg 4, 2628CD, Delft, Netherlands

[4] Fac. EE, National University of Defence Technology, 410073, Changsha, China

ABSTRACT

Since the global positioning system (GPS) is not applicable underwater, source localization using wireless sensor networks (WSNs) is gaining popularity in oceanographic applications. Unlike terrestrial WSNs (TWSNs) which uses electromagnetic signaling, underwater WSNs (UWSNs) require underwater acoustic (UWA) signaling. Received signal strength (RSS)-based source localization is considered in this paper due to its practical simplicity and the constraint of low-cost sensor devices, but this area received little attention so far because of the complicated UWA transmission loss (TL) phenomena. In this paper, we address this issue and propose two novel semidefinite programming (SDP) approaches which can be solved more efficiently. The numerical results validate our proposed SDP solvers in underwater environments, and indicate that the placement of the anchor nodes influences the RSS-based localization accuracy similarly as in the terrestrial counterpart. We also highlight that adopting traditional terrestrial RSS-based localization methods will fail in underwater scenarios.

Index Terms— Underwater, Localization, RSS-based, SDP.

1. INTRODUCTION

Underwater acoustic (UWA) communication systems differ from terrestrial telemetry due to differences in system geometry and environmental conditions [1]. Underwater wireless sensor networks (UWSNs) are envisioned for oceanographic applications such as pollution monitoring, offshore exploration, disaster prevention, assisted navigation, and tactical surveillance applications, while source localization is another important task. Apart from localization protocol designs [2], researchers paid a lot of attention to four different underwater distance measurement techniques [3] as applied in TWSNs, including time difference of arrival (TDoA), time of arrival (ToA), received signal strength (RSS), and angle of arrival (AoA). ToA is widely employed in underwater source localization works for measuring the distance, e.g., [4], although it demands a precise synchronization among nodes which is challenging in UWSNs. TDoA either uses two different transmission media (like
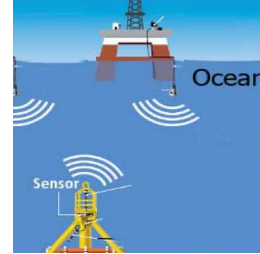
Fig. 1. Demonstration of UWA localization

radio and acoustic waves) or adopts reference beacons to estimate the distance. However, the former is infeasible since RF is not applicable in aquatic environments [5], while the latter can lead to problems due to the unpredictable UWA velocities [6]. AoA relies on a direct line-of-sight (LOS) UWA transmission path which may not exist at all unlike in terrestrial radio [7], while typical multi-path components in UWA channels can also lead to large errors in AoA measurements [8]. RSS-based underwater source localization gets less attention as another alternative to measure distance, since it is difficult to achieve accurate ranging due to multipath propagations and the complicated UWA transmission loss (TL) phenomena [3]. However, it can be argued that for certain water depths, the UWA channels show nice transmission features that fit well to a TL model and thus RSS-based localization can be considered for such cases [9]. To represent the TL features of an UWA channel, the Urick propagation model [10] is among the most popular, based on which some statistical models are derived [11]. Other UWA TL modeling methods can also be found, e.g., using Lambert W function [12]. In this paper, we consider RSS-based UWA localization using UWSNs, where the target is a source node that transmits acoustic signals to all the anchor nodes (beacons) which usually lie on the water surface and are able to obtain their precise locations via GPS as depicted in Fig. 1. Literature studying RSS-based localization underwater using acoustic waves is rather rare, yet it includes [9] choosing the Lambert W function to model the UWA TL and performing a simple triangulation method based on known distances, [13] combining TOA and RSS measurements where the RSS-based measurements are simply assumed known and [14] adopting a terrestrial acoustic wave propagation model to study RSS-based underwater localization. In this sense, we may for the first time introduce SDP solvers for UWA RSS-based localization in UWSNs based on a UWA propagation model.

Notation: Upper (lower) bold-face letters stand for matrices (vectors); superscript T denotes transpose, $[\mathbf{A}]_{k,m}$ stands for the (k,m)th entry of the matrix $\mathbf{A}$, $\mathrm{Trace}[\mathbf{A}]$ for the trace of the matrix $\mathbf{A}$, $\mathrm{Rank}[\mathbf{A}]$ for the rank of the matrix $\mathbf{A}$; $\mathbb{R}^M$ represents the M-

dimensional field of real numbers.

2. SYSTEM MODEL

Acoustic transmission loss (TL) in water is classified as spreading loss, including spherical and cylindrical, and attenuation loss consisting of absorption, duct leakage, scattering and diffraction. Generally, attenuation parameters relate to the medium (salinity, acidity, pressure, and temperature) and the environment (air bubbles, sediment absorption, surface reflection and scattering) [5]. The TL that a narrow-band acoustic signal centered at frequency f experiences along a distance $d > 0$ can be described in decibels (dB) as

$$\psi_{\text{TL}}(f, d) = 10\beta\log_{10}d + \alpha^{(f)}d + \xi^{(f,d)}, \qquad (1)$$

where the term $10\beta\log_{10}d$ accounts for geometric spreading which increases with the propagation distance and is independent of frequency, with $\beta \geq 0$ being the path-loss exponent (PLE); the term $\alpha^{(f)}d$ accounts for the frequency-dependent absorption by the medium in the Urick propagation model [15] with $\alpha^{(f)}$ being the absorption coefficient that can be obtained in dB per kilometer using Thorp's empirical formula as [11]

$$0.11\frac{f^2}{1+f^2} + 44\frac{f^2}{4100+f^2} + 2.75 \times 10^{-4}f^2 + 0.003, \quad (2)$$

while other formulae also exist [16]; the parameter $\xi^{(f,d)}$ can be viewed to contain other residual factors in the TL model, e.g., the reflection loss [16]. We notice that the deformation forms of the TL model (1) can be found widely in UWA research, e.g., (1) in [17], (1) in [11] and (8-32) in [18]. Utilizing the RSS as a measurement means that the average of the instantaneous received power is attained over several consecutive time slots and hence the small-scale fading can be neglected. Hence, we describe the RSS value $P_i^{(f)}$, measured using the frequency component f by the i-th anchor node located at $\mathbf{s}_i \in \mathbb{R}^M$ over a distance $d_i = \|\mathbf{x} - \mathbf{s}_i\|_2 > 0$ with the source node located at $\mathbf{x} \in \mathbb{R}^M$, using the following formula

$$P_i^{(f)} = P_0^{(f)} - (\psi_{\text{TL}}(f, d_i) - \psi_{\text{TL}}(f, d_0))$$
$$= P_0^{(f)} - 10\beta\log_{10}\frac{d_i}{d_0} - \alpha^{(f)}(d_i - d_0) + n_i^{(f)}, \quad (3)$$

where $P_0^{(f)}$ is the received power at the reference distance d_0 using the frequency component f, while $n_i^{(f)} = \xi_0^{(f,d0)} - \xi_i^{(f,d_i)}$, for $i = 1, 2, \cdots, N$ with N being the number of the anchor nodes. A similar model is adopted in [19]. It is noteworthy that when $\alpha^{(f)} \equiv 0$ as in [14], a popular RSS-based terrestrial localization scheme is obtained and classic RSS-based localization methods can be utilized [20].

From now, we choose $d_0 = 1$ for convenience. When the PLE β and the absorption coefficient $\alpha^{(f)}$ are assumed perfectly known, the most popular way to solve (3) is given by the following optimization problem [21]

$$\hat{\mathbf{x}}_{\text{basic}} = \operatorname*{argmin}_{\mathbf{x}\in\mathbb{R}^M}\sum_i^N (P_i^{(f)} + 10\beta\log_{10}d_i + \alpha^{(f)}d_i)^2, \quad (4)$$

which can align with the maximum likelihood (ML) estimator if $n_i^{(f)}$ is zero-mean Gaussian distributed. Unfortunately, we do not have such a guarantee about $n_i^{(f)}$ underwater. In any case, the solution of (4) cannot be formulated in closed-form and can only be approximated by iterative numerical techniques such as the Gauss-Newton method, whose drawback is that it requires a good initialization to make sure that the algorithm converges to the global minimum. Otherwise, the iterative solver can return a local minimum or saddle point with a large estimation error.

3. SEMIDEFINITE PROGRAMMING SOLOVER

In this section, our proposed estimators will be derived. As mentioned previously, the cost function in (4) is severely nonlinear and nonconvex [22], requiring involved computations. By using semidefinite relaxation (SDR), we convert the optimization problem into a convex semidefinite programming (SDP) problem. The advantage of the SDP problem over iterative solvers is that it can be solved with efficient computational methods that certainly converge to its global minimum [23].

3.1. RSS-based Approach

From (3), we approximately obtain

$$\lambda_i^{(f)}d_i^2 + \gamma_i^{(f)}d_i - 1 = \epsilon_i^{(f)}, \qquad (5)$$

where we refer the readers to the Appendix for the detailed derivations as well as for the expressions of $\lambda_i^{(f)}$ and $\gamma^{(f)}$ as well as $\epsilon_i^{(f)}$.

To solve (5), the straightforward method is again to minimize the ℓ_2 norm of the residual error. Specifically, we have

$$\operatorname*{argmin}_{\mathbf{x}\in\mathcal{R}^M}\sum_i^N (\lambda_i^{(f)}d_i^2 + \gamma^{(f)}d_i - 1)^2 \qquad (6)$$

which includes a quadratic polynomial form w.r.t. d_i, and hence it is very troublesome to handle. In addition, we do not have enough information about $n_i^{(f)}$ (also $\epsilon_i^{(f)}$)), which means that (6) may not lead to an ML estimate at all. Thus we are motivated to introduce the ℓ_1 norm instead of the ℓ_2 norm to formulate the underwater localization problem, leading to

$$\min_{\mathbf{x}\in\mathcal{R}^M}\sum_i^N \left|\lambda_i^{(f_k)}d_i^2 + \gamma^{(f)}d_i - 1\right| \qquad (7)$$

Note that replacing the ℓ_2 norm with the ℓ_1 norm for solving optimization problems can also be found in other work, e.g., in [24].

By introducing $d_i = \|\mathbf{x} - \mathbf{s}_i\|_2 > 0$ and the slack variable $t_i \geq 0$, we can convert the optimization problem (7) into

$$\min_{\mathbf{x},d_i,t_i}\sum_i^N t_i, \qquad (8a)$$

$$\text{s.t.} \quad -t_i < \lambda_i^{(f)}d_i^2 + \gamma^{(f)}d_i - 1 < t_i \qquad (8b)$$

$$d_i^2 = \|\mathbf{x} - \mathbf{s}_i\|_2^2 \qquad (8c)$$

For convenience, we now introduce the variables $\mathbf{X} \doteq \begin{bmatrix}\mathbf{x}\\1\end{bmatrix}\begin{bmatrix}\mathbf{x}^T & 1\end{bmatrix} = \begin{bmatrix}\mathbf{xx}^T & \mathbf{x}\\\mathbf{x}^T & 1\end{bmatrix}$ and $\mathbf{D} \doteq \begin{bmatrix}\mathbf{d}\\1\end{bmatrix}\begin{bmatrix}\mathbf{d}^T & 1\end{bmatrix} = \begin{bmatrix}\mathbf{dd}^T & \mathbf{d}\\\mathbf{d}^T & 1\end{bmatrix}$, where the vector $\mathbf{d}$ collects all values of d_i, such that the relations $\mathbf{x} = [\mathbf{X}]_{1:M,M+1}$, $d_i^2 = [\mathbf{D}]_{i,i}$ and $d_i = [\mathbf{D}]_{N+1,i}$ can be used later to facilitate our derivations. For example, the constraint (8c) can be converted into

$$[\mathbf{D}]_{i,i} = \begin{bmatrix}\mathbf{x}^T & 1\end{bmatrix}\begin{bmatrix}\mathbf{I}^T & -\mathbf{s}_i\\-\mathbf{s}_i^T & \mathbf{s}_i^T\mathbf{s}_i\end{bmatrix}\begin{bmatrix}\mathbf{x}\\1\end{bmatrix}$$
$$= \text{Trace}\,[\mathbf{X}\mathbf{S}_i] \qquad (9)$$

where $\mathbf{S}_i \doteq \begin{bmatrix}\mathbf{I}^T & -\mathbf{s}_i\\-\mathbf{s}_i^T & \mathbf{s}_i^T\mathbf{s}_i\end{bmatrix}$. However, $\mathbf{X}$ and $\mathbf{D}$ come with some more constraints since they are both positive semidefinite and $\text{Rank}(\mathbf{X}) = \text{Rank}(\mathbf{D}) = 1$.

After using the Schur complement to construct some linear matrix inequalities (LMIs), our optimization problem (8) is equivalent

to

$$\min_{\mathbf{D},\mathbf{X},t_i} \sum_i^N t_i, \tag{10a}$$

$$\text{s.t.} \quad -t_i < \lambda_i^{(f)} [\mathbf{D}]_{i,i} + \gamma^{(f)} [\mathbf{D}]_{N+1,i} - 1 < t_i \tag{10b}$$

$$[\mathbf{D}]_{i,i} = \text{Trace}\,[\mathbf{X}\mathbf{S}_i] \tag{10c}$$

$$\mathbf{X} \succeq \mathbf{0}, \; \mathbf{D} \succeq \mathbf{0} \tag{10d}$$

$$[\mathbf{X}]_{M+1,M+1} = [\mathbf{D}]_{N+1,N+1} = 1 \tag{10e}$$

$$\text{Rank}(\mathbf{X}) = \text{Rank}(\mathbf{D}) = 1 \tag{10f}$$

We now apply SDR by omitting the rank constraint (10f), leading to

$$\min_{\mathbf{D},\mathbf{X},t_i} \sum_i^N t_i, \tag{11a}$$

$$\text{s.t.} \quad -t_i < \lambda_i^{(f)} [\mathbf{D}]_{i,i} + \gamma^{(f)} [\mathbf{D}]_{N+1,i} - 1 < t_i \tag{11b}$$

$$[\mathbf{D}]_{i,i} = \text{Trace}\,[\mathbf{X}\mathbf{S}_i] \tag{11c}$$

$$\mathbf{X} \succeq \mathbf{0}, \; \mathbf{D} \succeq \mathbf{0} \tag{11d}$$

$$[\mathbf{X}]_{M+1,M+1} = [\mathbf{D}]_{N+1,N+1} = 1 \tag{11e}$$

which is an SDP optimization problem that converges to the global minimum [23], and our SDP-based estimate is given by $\hat{\mathbf{x}} = \left[\hat{\mathbf{X}}\right]_{1:M,M+1}$.

3.2. FDRSS-based Approach

So far, we have considered a single frequency component, e.g., f, and did not take advantage of the frequency-dependent features in (3). Now, we consider a differential RSS (DRSS) scheme by subtracting the RSS values in (3) according to two distinctive frequency components at each anchor, called the frequency-dependent DRSS (FDRSS) approach. Specifically, we have

$$P_i^{(\Delta)} = P_0^{(\Delta)} - \alpha^{(\Delta)}(d_i - d_0) + n_i^{(\Delta)}, \tag{12}$$

where $P_i^{(\Delta)} = P_i^{(f_k)} - P_i^{(f_p)}$, $P_0^{(\Delta)} = P_0^{(f_k)} - P_0^{(f_p)}$, $\alpha^{(\Delta)} = \alpha^{(f_k)} - \alpha^{(f_p)}$ and $n_i^{(\Delta)} = n_i^{(f_k)} - n_i^{(f_p)}$ for $k \neq p$. In such a FDRSS expression, the frequency-independent geometric spreading term in (3) is eliminated, and there are no approximation operations as in (17) and (18) any more. We argue that although $\alpha^{(f)}$ is usually small [11] and thus $P_i^{(\Delta)}$ may be too small to be sensible in practice, we can always quantify them by high-precision devices. Hence we rewrite (12) by taking $d_0 = 1$ as

$$\alpha^{(\Delta)} d_i - \eta_i^{(\Delta)} = n_i^{(\Delta)}, \tag{13}$$

where $\eta_i^{(\Delta)} = P_0^{(\Delta)} + \alpha^{(\Delta)} - P_i^{(\Delta)}$, and its estimate is given by

$$\operatorname*{argmin}_{\mathbf{x} \in \mathbb{R}^M} \sum_i^N (\alpha^{(\Delta)} \|\mathbf{x} - \mathbf{s}_i\|_2 - \eta_i^{(\Delta)})^2 \tag{14}$$

which can be solved by [20]

$$\min_{\mathbf{D},\mathbf{X}} \sum_i^N \left(\alpha^{(\Delta)^2} [\mathbf{D}]_{i,i} - 2\alpha^{(\Delta)} \eta_i^{(\Delta)} [\mathbf{D}]_{N+1,i} + \eta_i^{(\Delta)^2} \right), \tag{15a}$$

$$\text{s.t.} \quad [\mathbf{D}]_{i,i} = \text{Trace}\,[\mathbf{X}\mathbf{S}_i] \tag{15b}$$

$$\mathbf{X} \succeq \mathbf{0}, \; \mathbf{D} \succeq \mathbf{0} \tag{15c}$$

$$[\mathbf{X}]_{M+1,M+1} = [\mathbf{D}]_{N+1,N+1} = 1 \tag{15d}$$

which is also a SDP solver and the definitions of $\mathbf{D}$, $\mathbf{X}$ and $\mathbf{S}_i$ are the same as in (11), while the estimate is given by $\hat{\mathbf{x}} = \left[\hat{\mathbf{X}}\right]_{M+1,1:M}$.

4. COMPUTER SIMULATIONS AND DISCUSSIONS

In this section, we perform a number of computer simulations to demonstrate the performance of the proposed methods. The RSS values according to each frequency component are obtained according to (3) with $d_0 = 1$, where $\beta = 2$ corresponds to an UWA spherical spreading case [17]. We select a number of frequency components and obtain the related $\alpha^{(f)}$ according to (2). For instance, $\alpha^{(f_1)} \simeq 0.001$ dB per meter when $f_1 = 9$ kHz and $\alpha^{(f_2)} \simeq 0.01$ dB per meter when $f_2 = 34$ kHz, both of which are adopted for far distance UWA propagation in reality, while $\alpha^{(f_3)} \simeq 0.1$ dB per meter at $f_3 = 454$ kHz.

For simplicity, we adopt $M = 2$ (i.e., $\mathbf{x} \in \mathbb{R}^2$ and $\mathbf{s}_i \in \mathbb{R}^2$) and assume that $n_i^{(f)}$ in (3) is a zero-mean Gaussian random variable spatially correlated with covariance matrix $\mathbf{W}^{(f)}$ specified by $\left[\mathbf{W}^{(f)}\right]_{i,j} = \rho_{i,j}^{(f)} \sigma^{(f)^2}$, where $\sigma^{(f)}$ is the standard deviation which is constant with distance, while $\rho_{i,j}^{(f)}$ is the correlation coefficient between the ith and the jth links such that $\rho_{i,i}^{(f)} = 1$ for $i = 1, 2, \cdots, N$ and $\rho_{i,j}^{(f)} > 0$ for $i \neq j$. Such spatial correlation is also widely witnessed in terrestrial shadowing, e.g., in [25]. Fig. 2 depicts the cost functions related to the models in (4) and (7), which indicates that since the target node cannot overlap with the anchor nodes, every location of the anchor node becomes a singular point in (4) yielding multiple minima, while the counterpart in (7) is more smooth and has only a single optimal point.

We have conducted a Monte Carlo (MC) simulation using 1000 trials on a 100m × 100m field, where one target node and $N = 10$ anchor nodes are randomly deployed for each trial. The variance of $n_i^{(f)}$ is assumed to be $\sigma^{(f)^2} \in [-8, 10]$ [dB] and $\rho_{i,j}^{(f)} \equiv 0.6$ when $i \neq j$ for all frequencies. Fig. 3 describes the root mean square error (RMSE) to evaluate the performance of our estimators, which validates our proposed SDP solvers. Specifically, it explicates that the performance of our RSS-based SDP solver deteriorates with an increasing $\alpha^{(f)}$ and/or $n_i^{(f)}$, because of the higher approximation errors induced by (17) and (18), respectively. In this figure, we also give the RMSE result of our RSS-based approach when $\alpha^{(f)} = 0.1$ for the channel setup but we deliberately discard $\lambda_i^{(f)}$, i.e., $\lambda_i^{(f)} = 0$ in (11), to represent the case of adopting a traditional terrestrial RSS-based localization method for UWA scenarios. Not surprisingly, it yields the worst RMSE result in this test as shown in Fig. 3, because discarding the effect of the absorption coefficient (i.e., $\lambda_i^{(f)}$) during the localizing operation can be viewed as replacing (18) with a bad approximation given by $10^{\frac{\alpha(f) d_i}{10\beta}} \simeq 1$, which is unacceptable. It also implies that using a standard solver for a terrestrial RSS-based localization problem cannot be simply adopted for an underwater environment. In Fig. 3, the performance of our FDRSS-based solver is also validated with $\alpha^{(f_1)} = 0.001$ and $\alpha^{(f_2)} = 0.1$. It indicates that a better result of the FDRSS-based approach is yielded than the RSS-based approach since there are no approximation operations as in (17) and (18).

We also have conducted a MC simulation using 1000 trials on a 100m × 100m field, where one target node is randomly deployed for each trial but N anchor nodes are fixed at the surface of the water column, i.e., the y-coefficient for each $\mathbf{s}_i$ equals 100m for $i = 1, 2, \cdots, N$. Herein, we fix $\alpha^{(f)} = 0.01$ and keep $n_i^{(f)}$ the same as in the previous test. We consider two cases where we place $N = 4$ and $N = 8$ anchors, respectively, by uniformly distributing their x-coefficients within $[0, 100\text{m}]$; For the third case, we place $N = 8$ anchors but constrain their x-coefficients to the
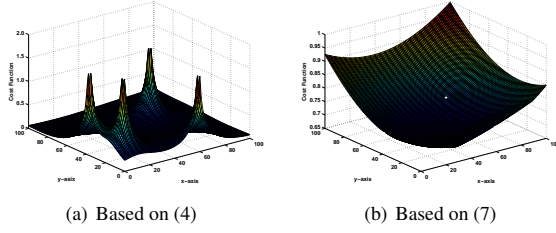
(a) Based on (4) (b) Based on (7)

Fig. 2. Comparison between the cost functions related to the models in (4) and (7) with $N = 4$ anchor nodes located at (59; 62), (35; 5), (10; 40) and (26; 1) while the target node is at (50; 50) on a 100×100 field in $\mathbb{R}^2$; $\sigma^{(f)^2} = 10$ [dB] and $\rho_{i,j}^{(f)} \equiv 0.6$ for $i \neq j$.
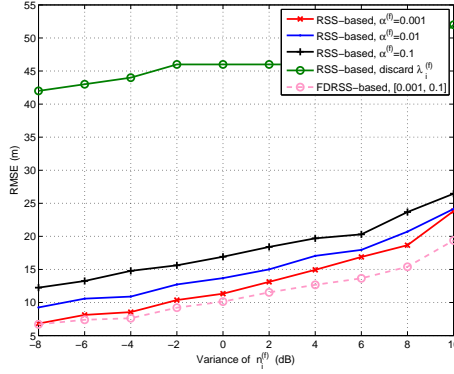

Fig. 3. Performance comparison under different channel setups

range $[80\mathrm{m}, 100\mathrm{m}]$. The RMSE results of these three cases are shown in Fig. 4 where we have adopted our SDP solver from (11). It is clear that the placement of the anchors influences the RSS-based localization accuracy. The distributed placement clearly yields a better performance than the clustered placement in this test. It also tells that more anchors can help accelerate the localization accuracy.
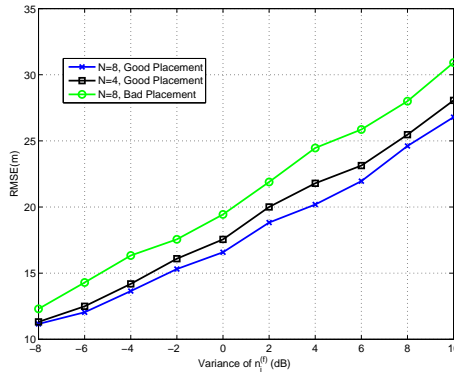

Fig. 4. Performance comparison with different anchor placements

5. CONCLUSIONS

RSS-based localization for underwater wireless sensor networks using acoustic signals has been introduced and studied. Based on a popular UWA transmission loss (TL) model, we have proposed and analyzed novel semidefinite programming (SDP) estimators, including an RSS-based approach and a frequency-dependent differential method called the FDRSS-based approach, both of which yield desirable localization performances. By numerical results, we have pointed out that using a standard solver for terrestrial RSS-based scenarios will fail in underwater cases, and the placement of the anchors matters for the underwater RSS-based localization accuracy. Future work includes studies on the optimal placement of underwater anchors, the impact of real-life underwater ambient noises, as well as model parameter estimation for the underwater TL model.

6. APPENDIX

To obtain (5), we rearrange (3) with $d_0 = 1$ and then divide it by 10β, giving

$$\frac{P_i^{(f)} - P_0^{(f)} - \alpha^{(f)}}{10\beta} + \log_{10} d_i + \frac{\alpha^{(f)}}{10\beta} d_i = \frac{n_i^{(f)}}{10\beta}$$

Taking the power of 10 on both sides yields

$$10^{\frac{P_i^{(f)} - P_0^{(f)} - \alpha^{(f)}}{10\beta}} \times d_i \times 10^{\frac{\alpha^{(f)} d_i}{10\beta}} = 10^{\frac{n_i^{(f)}}{10\beta}}. \quad (16)$$

When $n_i^{(f)}$ is sufficiently small ($|n_i^{(f)}| \ll 10\beta/\ln 10$) which is also widely adopted for terrestrial shadowing, we are allowed to use the first-order Taylor series expansion, approximately yielding

$$10^{\frac{n_i^{(f)}}{10\beta}} \simeq 1 + \frac{\ln 10}{10\beta} n_i^{(f)}. \quad (17)$$

We argue that $n_i^{(f)} = \xi_0^{(f,1)} - \xi_i^{(f,d_i)}$ can be sufficiently small especially in deep water environments where the reflection loss can ignored [18]. Similarly, we use

$$10^{\frac{\alpha^{(f)} d_i}{10\beta}} \simeq 1 + \frac{\ln 10}{10\beta} \alpha^{(f)} d_i, \quad (18)$$

since it is known that the absorption term $\alpha^{(f)} d_i$ can be relatively small [11] ($\alpha^{(f)} d_i \ll 10\beta/\ln 10$) especially in deep water. We then substitute (17) and (18) into (16) resulting in

$$\gamma_i^{(f)} \times d_i \times \left(1 + \frac{\alpha^{(f)} \ln 10}{10\beta} d_i\right) = 1 + \frac{\ln 10}{10\beta} n_i^{(f)} \quad (19)$$

with

$$\gamma_i^{(f)} = 10^{\frac{P_i^{(f)} - P_0^{(f)} - \alpha^{(f)}}{10\beta}}.$$

We can then shorten (19) to be

$$\lambda_i^{(f)} d_i^2 + \gamma_i^{(f)} d_i - 1 = \epsilon_i^{(f)}$$

which gives (5) with

$$\lambda_i^{(f)} = \frac{\gamma_i^{(f)} \alpha^{(f)} \ln 10}{10\beta}$$

and

$$\epsilon_i^{(f)} = \frac{\ln 10}{10\beta} n_i^{(f)}.$$

7. REFERENCES

[1] T. Xu, Z. Tang, G. Leus, and U. Mitra. Multi-rate block transmission over wideband multi-scale multi-lag channels. *IEEE Transactions on Signal Processing*, 4(61):964979, 2013.

[2] H. Ramezani, F. Fazel, M. Stojanovic, and G. Leus. Collision tolerant and collision free packet scheduling for underwater acoustic localization. *IEEE Transactions on Wireless Communications*, 1:1–12, 2015.

[3] H.-P. Tan, R. Diamant, W. K. G. Seah, and M. Waldmeyer. A survey of techniques and challenges in underwater localization. *Ocean Engineering*, 38:16631676, 2011.

[4] P. Carroll, S. Zhou, H. Zhou, X. Xu, J.-H. Cui, and P. Willett. Underwater localization and tracking of physical systems. *Journal of Electrical and Computer Engineering*, 2012:8, 2012.

[5] W.S. Burdic. *Underwater Acoustic System Analysis*. Peninsula Publishing, 2002.

[6] H. Ramezani and G. Leus. Ranging in an underwater medium with multiple isogradient sound speed profile layers. *Sensors*, 12:2996–3017, 2012.

[7] L.E. Emokpae, S. DiBenedetto, B. Potteiger, and M. Younis. UREAL: Underwater reflection-enabled acoustic-based localization. *IEEE Sensors Journal*, 14(11):3915–3925, 2014.

[8] G. Mao, B. Fidan, and B. D. Anderson. Wireless sensor network localization techniques. *Computer Networks*, 51(10):2529–2553, 2007.

[9] M. Hosseini, H. Chizari, and A. S. Ismail. New hybrid RSS-based localization mechanism for underwater wireless sensor networks. *International Journal of Computer Communications and Networks*, 1:1–10, 2011.

[10] R. J. Urick. *Principles of Underwater Sound*. McGraw-Hill, 1983.

[11] P. Qarabaqi and M. Stojanovic. Statistical characterization and computationally efficient modeling of a class of underwater acoustic communication channels. *IEEE J. Oceanic. Eng.*, 38(4):701–717, 2013.

[12] M. Hosseini, H. Chizari, T. Poston, M. B. Salleh, and Abdullah A. H. Efficient underwater RSS value to distance inversion using the Lambert function. *Mathematical Problems in Engineering*, 2014:8, 2014.

[13] C Kim, S. Lee, and K. Kim. 3D underwater localization with hybrid ranging method for near-sea marine monitoring. In *Proc. Int. Conf. Embedded and Ubiquitous Computing (EUC)*, pages 438–441, 2011.

[14] Y. Yan, W. Wang, X. Shen, F. Yang, and Z. Chen. Efficient convex optimization method for underwater passive source localization based on RSS with WSN. In *Proc. Int. Conf. Signal Processing, Communication and Computing (ICSPCC)*, pages 171–174, 2012.

[15] M. C. Domingo. Overview of channel models for underwater wireless communication networks. *Physical Communication*, 1(3):163–182, 2008.

[16] B. Zhang. Underwater acoustic channel modeling. Master's thesis, State University of New York, Buffalo city, 2011.

[17] D. Pompili and I. F. Akyildiz. A multimedia cross-layer protocol for underwater acoustic sensor networks. *IEEE Transactions on Wireless Communications*, 9(9):2924–2933, 2010.

[18] *Fundamentals of Naval Weapons Systems: Chapter 8*. Weapons and Systems Engineering Department of United States Naval Academy, 1989.

[19] H.-P. Diamant, R.and Tan and L. Lampe. LOS and NLOS classification for underwater acoustic localization. *IEEE TRANSACTIONS ON MOBILE COMPUTING*, 13(2):311–323, 2014.

[20] A. Beck and J. Stoica, P. andLi. Exact and approximate solutions of source localization problems. *IEEE Transactions on Signal Processing*, 56(5):1770–1778, 2008.

[21] S. M. Kay. *Fundamentals of Statistical Signal Processing: Estimation Theory*. Prentice Hall, 1993.

[22] R. Ouyang, A.-S. Wong, and C.-T. Lea. Received signal strength-based wireless localization via semidefinite programming: Noncooperative and cooperative schemes. *IEEE Trans. Veh. Technol.*, 59(3):1307–1318, 2010.

[23] S. Boyd and L. Vandenberghe. *Convex Optimization*. Cambridge University Press, 2004.

[24] R. M. Vaghefi, M. R. Gholami, and E. G. Strom. RSS-based sensor localization with unknown transmit power. In *Proc. ICASSP 2011*, pages 2480–2483, 2011.

[25] R. M. Vaghefi and R. M. Buehrer. Received signal strength-based sensor localization in spatially correlated shadowing. In *Proc. ICASSP 2013*, pages 1–5, 2013.